Supplementary Information

Changing Northern Hemisphere Weather Linked to Warming Amplification in High Mountain Asia

Yongkun Xie, Jianping Huang*, Guoxiong Wu*, Jiaqin Mi, Yimin Liu, Zifan Su, Yuzhi Liu, Xiaodan Guan

* Corresponding authors. Email: hjp@lzu.edu.cn, gxwu@lasg.iap.ac.cn

This PDF file includes:

Figures S1 to S6

Table S1

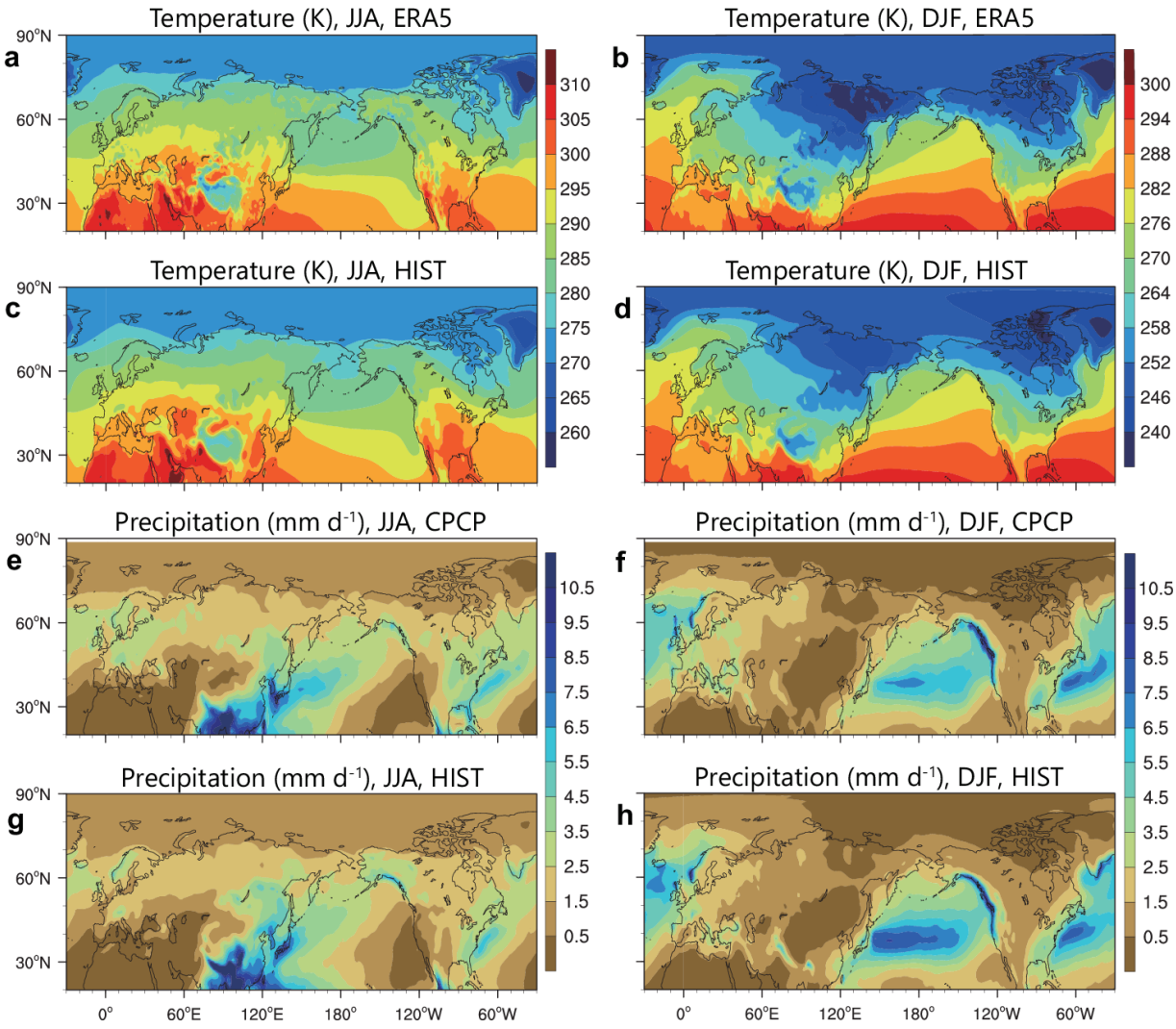

Fig. S1. Climatology of temperature and precipitation. Near-surface air temperature averaged from 1980 to 2010 in (**a**) June to August (JJA) and (**b**) December to February (DJF), based on ERA5 reanalysis data. (**c**, **d**) Same as (a, b) but for the HIST experiment from 1980 to 2010. (**e**–**h**) Same as (a–d) but for precipitation.

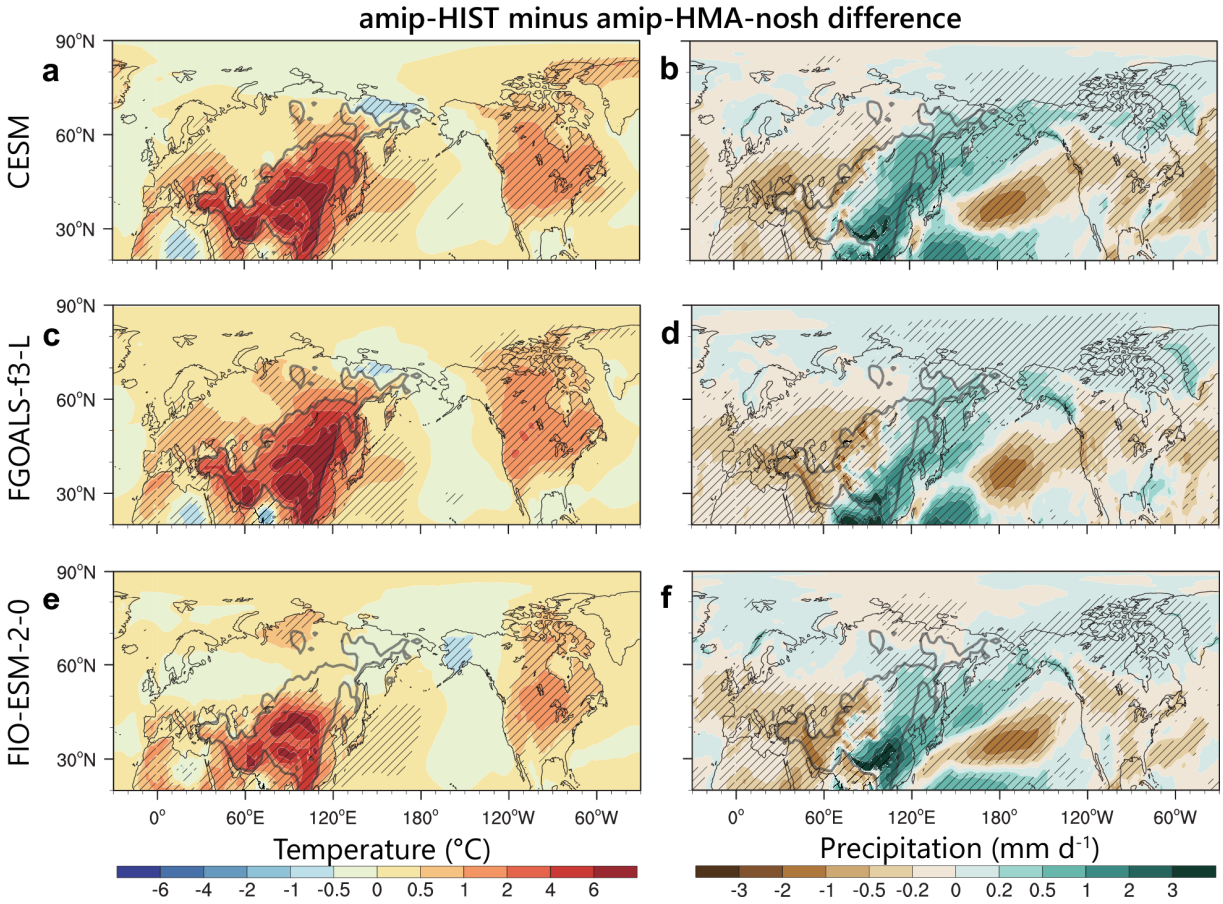

Fig. S2. Temperature and precipitation responses in atmosphere-only experiments. Differences in annual mean near-surface air temperature from 1979 to 2014 determined using amip-HIST minus amip-HMA-nosh experiments from (**a**) CESM, (**c**) FGOALS-f3-L, and (**e**) FIO-ESM-2-0 models. The stripes indicate significant differences between two experiments at the 95% ($P < 0.05$) confidence level based on the two-tailed Student's t-test. (**b**, **d**, **f**) Same as (a, c, e) but for precipitation.

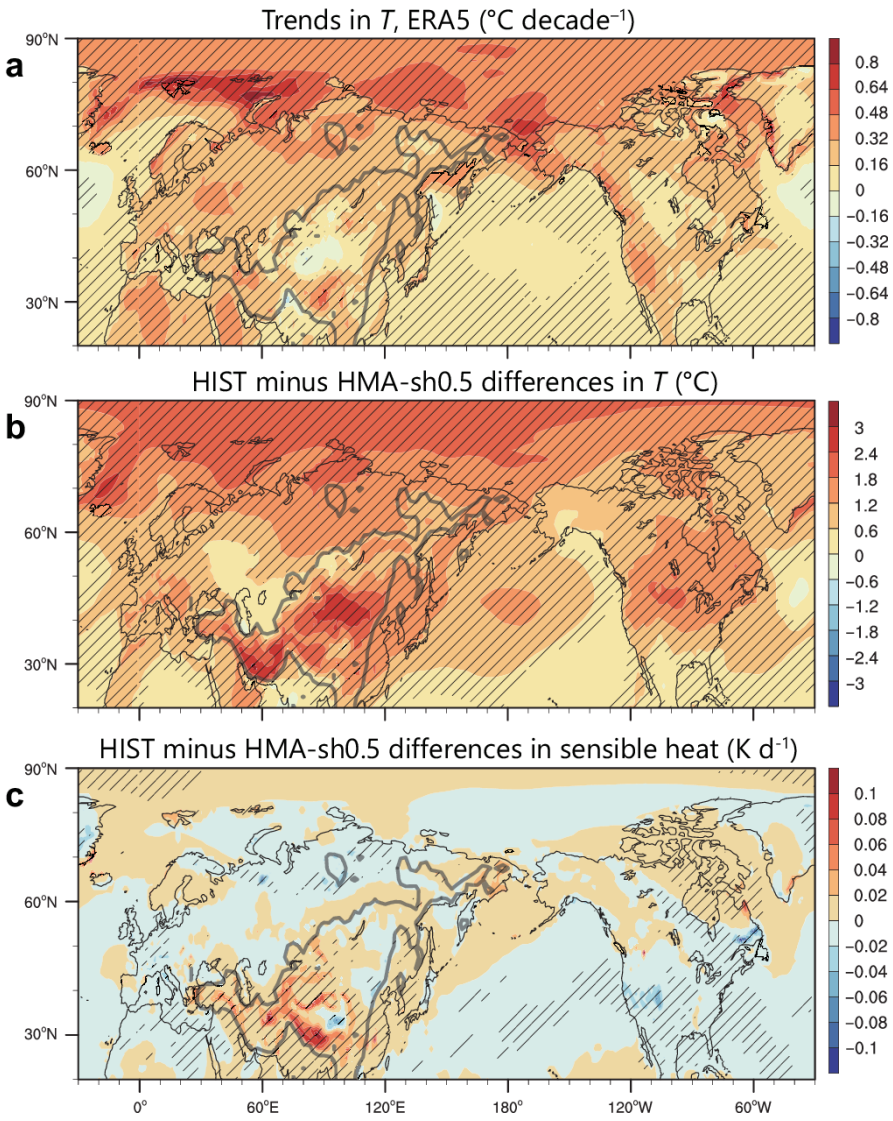

Fig. S3. Temperature trends in observations and HMA warming-induced temperature changes in simulations. (**a**) Linear trends in annual mean near-surface air temperature (T) from 1940 to 2022 based on ERA5 data. The stripes indicate significant trends at the 95% ($P_{adj} < 0.05$) confidence level based on the two-tailed Student's t-test and false discovery rate (FDR)-adjusted P-values (P_{adj}). (**b**) Differences in annual mean T for 2000–2014 determined from ensemble means of HIST minus HMA-sh0.5 experiments. The stripes indicate significant differences between HIST and HMA-sh0.5 at the 95% ($P < 0.05$) confidence level based on the two-tailed Student's t-test. (**c**) Same as (b) but for diffusive sensible heat at the lowest model level.

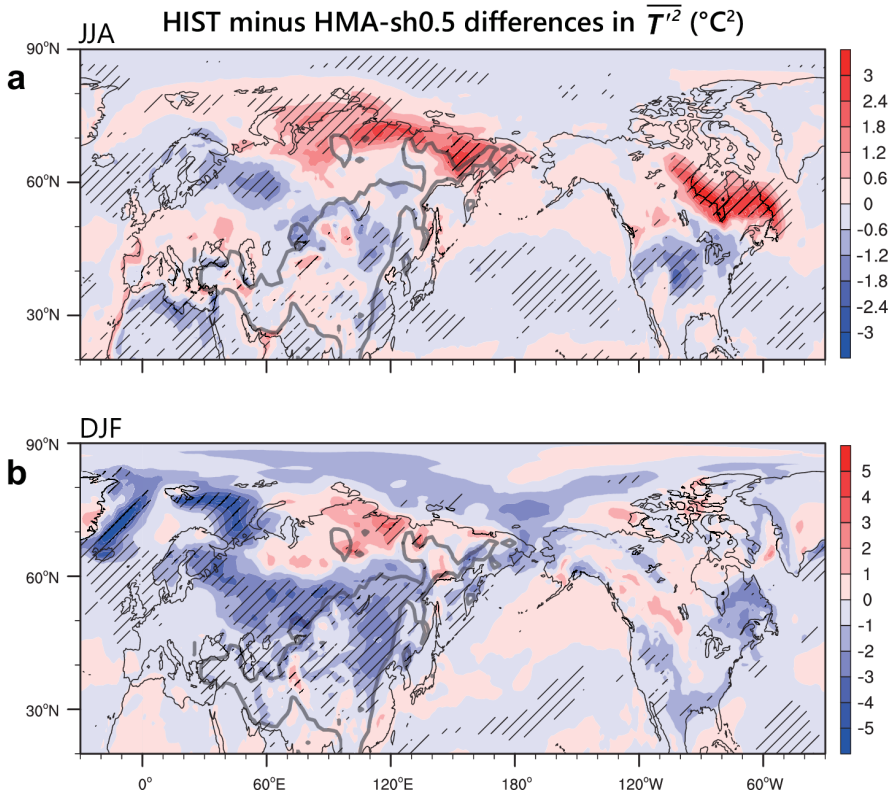

Fig. S4. HMA warming-induced changes in STV. Differences in STV ($\overline{T'^2}$) attributable to HMA warming (2000–2014) in (**a**) JJA and (**b**) DJF, derived from HIST minus HMA-sh0.5 experiments. Striped areas indicate significant differences ($P < 0.05$, two-tailed Student's t-test).

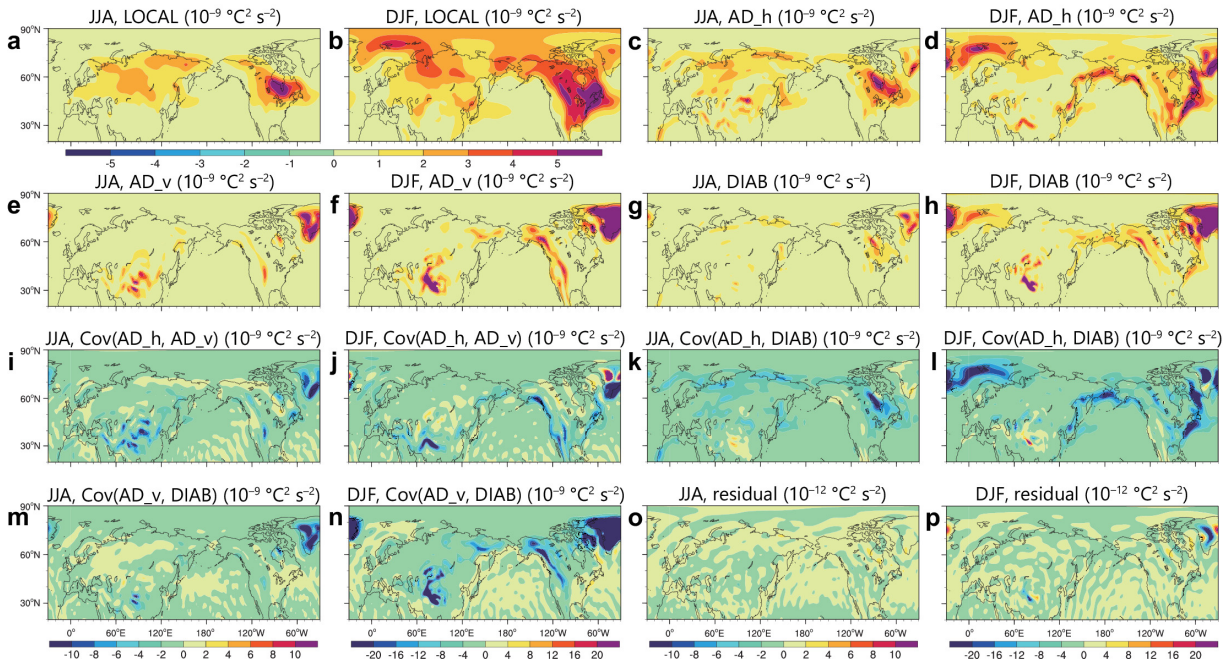

Fig. S5. Physical processes governing climatological patterns of STV. Synoptic temperature tendency (T_{tend}) variance (**a**, **b**; LOCAL) due to adiabatic horizontal temperature advection (**c**, **d**; AD_h), adiabatic vertical motion-induced temperature modification (**e**, **f**, AD_v), diabatic process (**g**, **h**; DIAB), and their covariance (**i–n**; Cov) according to Eq. (8), for 2000–2014 ensemble mean of HIST experiment, in JJA and DJF, respectively. (**o**, **p**) The residual term calculated as the left-hand side minus the sum of right-hand side terms in Eq. (8), with magnitudes three orders of magnitude smaller than (a–n).

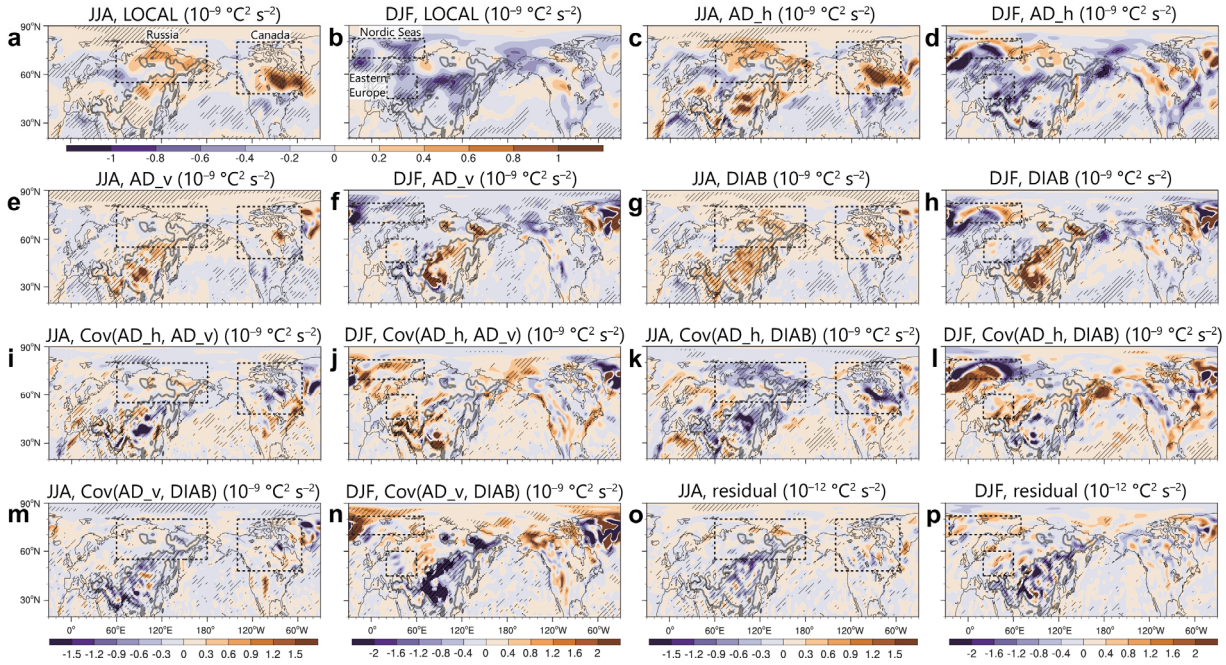

Fig. S6. Physical process contributions to HMA warming-induced STV changes. Differences in synoptic temperature tendency (T_{tend}) variance (**a**, **b**; LOCAL) due to adiabatic horizontal temperature advection (**c**, **d**; AD_h), adiabatic vertical motion-induced temperature modification (**e**, **f**; AD_v), diabatic process (**g**, **h**; DIAB), and their covariance (**i–n**; Cov) according to Eq. (8) based on ensemble means from numerical experiments (HIST minus HMA-sh0.5) for 2000–2014, in JJA and DJF, respectively. Striped regions indicate statistically significant differences ($P < 0.05$, two-tailed Student's t-test). (**o**, **p**) The residual term calculated as the left-hand side minus the sum of right-hand side terms in Eq. (8), with magnitudes three orders of magnitude smaller than (a–n).

Table S1. Information on model and experimental designs. Red shading denotes models/experiments used in this study, while blue indicates GMMIP-provided experiments.

Model used in this study		
Name	Resolution	Institute
CESM (version 2.1.3)	Official tag: f09_g17[a]. Atmos: CAM6, 0.9 × 1.25 finite volume grid, 32 vertical levels. Land: CLM5.0, 0.9 × 1.25 finite volume grid. Ocean: POP2, finite volume grid 0.9 × 1.25_g × 1v7.	NCAR & UCAR, United States of America
Experiments performed		
Name	Design description	Time
HIST (control)	The control run was the benchmark CMIP6 historical (HIST) simulation, with external forcing defined by the observed values. Modified from the official case: BHIST[b].	Ensemble 1: 1850/01–2014/12 (three-hourly outputs only for 2000/01–2014/12) Ensembles 2, 3: 2000/01–2014/12 (initialized by 1998, 1999 conditions)
HMA-sh0.5	The sensitivity run was modified from HIST. The diabatic heating of HMA was modified by halving the diffusive sensible heat throughout the entire column of the atmosphere at each model integration time step. This modification maintains full land-atmosphere coupling and feedback processes.	
amip-HIST	Atmosphere-only historical simulation with prescribed sea surface temperatures (no active ocean coupling).	1979/01–2014/12
amip-HMA-nosh	Same as HMA-sh0.5 but for atmosphere-only simulation.	

GMMIP models		
Name	Resolution	Institute
FGOALS-f3-L	Atmos: FAMIL2.2, c96 finite volume grid; 180 × 360 lat/lon; 32 vertical levels.	IAP-LASG, China
FIO-ESM-2-0	Atmos: CAM4, 0.9 × 1.25 finite volume grid; 192 × 288 lat/lon; 26 vertical levels.	FIO, China
GMMIP experiments		
Name	Design description	Time
amip-HIST	These experiments followed the same configurations as their CESM counterparts (amip-HIST and amip-HMA-nosh) but used different integration periods. In GMMIP nomenclature: The atmosphere-only historical run was tagged as "amip-hist", while the no-sensible-heat experiment was tagged as "amip-TIP-nosh", where TIP denotes the Tibetan-Iranian Plateau coupling system.	1861/01–2014/12
amip-HMA-nosh		1870/01–2014/12

[a] https://docs.cesm.ucar.edu/models/cesm2/config/2.1.3/grids.html
[b] https://docs.cesm.ucar.edu/models/cesm2/config/2.1.3/compsets.html